

Analyst

Accepted Manuscript



This is an *Accepted Manuscript*, which has been through the Royal Society of Chemistry peer review process and has been accepted for publication.

Accepted Manuscripts are published online shortly after acceptance, before technical editing, formatting and proof reading. Using this free service, authors can make their results available to the community, in citable form, before we publish the edited article. We will replace this *Accepted Manuscript* with the edited and formatted *Advance Article* as soon as it is available.

You can find more information about *Accepted Manuscripts* in the [Information for Authors](#).

Please note that technical editing may introduce minor changes to the text and/or graphics, which may alter content. The journal's standard [Terms & Conditions](#) and the [Ethical guidelines](#) still apply. In no event shall the Royal Society of Chemistry be held responsible for any errors or omissions in this *Accepted Manuscript* or any consequences arising from the use of any information it contains.

Impedimetric transduction of swelling in pH-responsive hydrogels

Cite this: DOI: 10.1039/x0xx00000x

Nicky Mac Kenna,^a Paul Calvert^b and Aoife Morrin^a

Received 00th January 2012,
Accepted 00th January 2012

DOI: 10.1039/x0xx00000x

www.rsc.org/

A pH-responsive hydrogel composed of an aliphatic diamine cross-linked with polyethylene glycol diglycidyl ether (PEGDGE) using a single, rapid polymerisation step has been used to detect glucose by entrapping glucose oxidase (GOx) within its cationic network. The swelling response of hydrogel disks on exposure to glucose were optimised through variation of factors including the cross-linking density of the network, GOx loading and the addition of catalase. Hydrogel-modified carbon cloth electrodes were also prepared and characterised using voltammetric and impedimetric techniques. Non-faradaic electrochemical impedance spectroscopy (EIS) and gravimetry were both employed to track the swelling response of the gels quantitatively. The clear potential of utilising impedance to transduce hydrogel swelling was demonstrated where a linear decrease in gel resistance (R_{gel}) corresponding to the swelling response was observed in the range 1 to 100 μ M. A dramatic increase in the limit of detection of six orders of magnitude over the gravimetric measurement was achieved (from 0.33 mM to 0.08 μ M). This increased sensitivity, coupled with the textile-based electrode substrate approach opens the potential applicability of this system for monitoring glucose concentration via the skin by sweat or interstitial fluid (ISF).

Introduction

In recent years hydrogels have gained considerable attention as attractive materials in biosensing and diagnostic applications. These versatile materials have a high water content, unique swelling properties and often exhibit excellent biocompatibility. They possess many biological traits resembling natural living tissue both compositionally and mechanically^{1, 2}. In sensing applications, hydrogels have predominantly been used as a support material for the immobilisation of biomolecules. Their 3D matrix enables an increased loading capacity versus 2D immobilisation, whilst providing stability and protection to the active part of the sensor. Alternatively, hydrogel specific properties (swelling, phase transitions⁷ etc.) are also being exploited. In particular, stimuli-sensitive hydrogels, which experience large reversible transitions in their swelling behaviour due to small environmental changes, have received increasing interest. These hydrogels can be designed to support signal transduction via swelling in response to a wide variety of chemical stimuli including pH³, temperature⁴, light⁵, specific ions⁶⁻⁸, humidity or solvents⁹, electric or magnetic fields^{10, 11}, chemical or biological agents¹² etc. Some hydrogels are designed to respond to multiple stimuli¹³⁻¹⁵. Upon appropriate stimulation, the induced swelling produces conformational changes which alter many properties of the hydrogel system;

including network structure, permeability, refractive index, interfacial tension and mechanical strength^{16, 17}. These intelligent materials are capable of sensing a particular change in the local environment, transducing it and in some instances responding e.g. titrated drug or reagent delivery into that environment to offset the environmental change.

Commonly used transduction systems for hydrogel swelling are based on optical and mechanical methods¹⁸. They function by detecting changes in the properties of the polymer network, including cross-linking density, volume and tensile strength, or on the mechanical work produced by the swelling mechanism¹⁹. Electrochemical transduction is frequently used in chemical and biochemical sensing given its reliability, direct coupling with microelectronics, facilitated quantitative control and ease of interfacing with intricate systems. It offers the possibility of mass production of low cost, disposable electrode devices amenable to miniaturisation and widespread application.

Voltammetry and EIS are used routinely in the characterisation and optimisation of the role of hydrogels and hydrogel-encapsulated materials in sensors. These techniques provide information about electron transfer kinetics and the stability of reactions for optimising hydrogel design. Numerous amperometric biosensors have been fabricated using passive hydrogels as encapsulation media²⁰, stimuli-sensitive hydrogels capable of tuning the sensor characteristics²¹, electroconductive

hydrogels²²⁻²⁴ and redox hydrogels in which redox polymers are crosslinked or 'wired' to the redox centres of enzymes²⁵⁻²⁷. To date EIS has been employed in the investigation of the influence of film thickness of a thin coating of poly(hydroxyethylmethacrylate) (pHEMA) on an impedance biosensor array²⁸, to assess the effect of voltage on liposome stability within poly(vinyl alcohol) hydrogels²⁹, to investigate the applications of coatings onto hydrogel contact lenses³⁰ and to study the swelling mechanism of conducting polymer matrices in response to doping³¹ among other applications. Little research has been done to date on using an electrochemical or electrical transduction method to quantitatively track hydrogel swelling in response to a particular analyte for a sensor application^{32, 33}.

The application of hydrogels as a sensing platform for glucose has gained considerable interest in recent years. Three distinct classes of glucose-sensitive hydrogels exist; phenylboronic acid-containing, lectin-loaded and glucose-oxidase loaded hydrogels. Many researchers have exploited the high affinity of phenylboronic acid for complexing with glucose³⁴⁻³⁶. However, phenylboronic acid is often most sensitive to glucose in alkaline conditions and can potentially be unstable at physiological pH. Several other investigations have focussed on the complementary binding of a lectin (concanavalin A) to glucose³⁷⁻³⁹. Also, lectin systems can be limited by the leaching of concanavalin A leading to a progressive loss in activity and immunotoxicity issues⁴⁰.

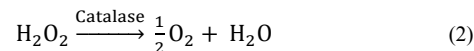
This work describes the fabrication and characterisation of a glucose biosensor based on the swelling response of a pH sensitive hydrogel. The swelling is tracked using both gravimetric and impedimetric means. The hydrogel comprises an aliphatic diamine crosslinked with polyethylene glycol diglycidyl ether (PEGDGE) in a single simple polymerization step, generating a polymeric network with pendant basic groups. GOx was entrapped within the ionisable gel network to target glucose as a model analyte. The enzymatic catalysis of glucose produces gluconic acid as follows:



The protons produced by the partial dissociation of gluconic acid ionise the pendant basic groups of the hydrogel network and generate charge along the polymer backbone. Electrostatic repulsion forces between adjacent ionized groups create a large swelling force altering the hydrodynamic volume and permeability of the gel. Additionally, gluconate anions migrate into the gel matrix to balance the charge, producing additional osmotic pressure and increasing the swelling capacity further. The effect of these network volume changes on analyte diffusion were detected and monitored using voltammetry of a bulk solution redox probe and non-faradaic EIS.

The hydrogel system was studied in the presence of catalase. Two inherent limitations of glucose-based sensors can be at least partially overcome by the inclusion of catalase. Oxygen availability is one of these limitations because of the

low solubility of oxygen in aqueous-based solutions. As seen in Equation 1, one mole of oxygen is required to react with one mole of glucose in the enzymatic catalysis of glucose. Additionally, hydrogen peroxide production during the catalysis is known to inhibit the activity of GOx⁴³. Catalase can catalyse hydrogen peroxide and produce oxygen according to Equation 2:



According to this equation, catalase produces half a mole of oxygen reducing the oxygen limitation of the GOx enzymatic reaction and the hydrogen peroxide inhibition. This enhancement is necessary for long-term glucose monitoring. As such, the incorporation of catalase into this system was studied.

Carbon cloth was selected as a suitable electrode material for investigating the swelling response of the hydrogel due to its high porosity and flexibility. These characteristics provide extra support to the swollen hydrogel, reducing the risk of delamination from the electrode surface, without restricting the swelling response. This use of a textile-based approach coupled with the detection sensitivity of EIS suggests the potential of this system for skin analysis of glucose.

Materials and Methods

Materials

Poly (ethylene glycol) diglycidyl ether (PEGDGE, average Mn 526), glucose oxidase from *Aspergillus niger* (GOx, 17,300 U/g), catalase from *Aspergillus niger* (480,947 U/g), D-gluconic acid solution and potassium ferrocyanide (II) trihydrate ($\text{K}_4[\text{Fe}(\text{CN})_6] \cdot 3\text{H}_2\text{O}$) were purchased from Sigma-Aldrich (Ireland). Jeffamine[®] EDR-148 polyetheramine was obtained from Huntsman Corporation (US). D-glucose anhydrous was obtained from BDH Limited (UK). Untreated carbon cloth (44 x 48 yarns/inch, 99% carbon) was purchased from Fuel Cell Store (US) and phosphate buffer saline (PBS) tablets were purchased from Applichem (Germany). All chemicals were used as purchased and all aqueous solutions were prepared using ultrapure deionised (DI) water (18 MΩ cm @ 298 K). The Ag/AgCl reference electrode and Pt gauze auxiliary electrode were purchased from CH Instruments, Inc. (UK) and Sigma-Aldrich (Ireland) respectively.

Instrumentation

All electrochemical protocols were performed on a CH potentiostat (CHI660C), using cyclic voltammetry (CV) or AC impedance modes. Voltammetric studies were conducted in a potassium ferricyanide solution (2 mM) in KCl (1 M). The potential of the working electrode was cycled from -0.1 to 0.6 V vs. Ag/AgCl at a scan rate of 0.05 Vs⁻¹.

Electrochemical Impedance Spectroscopy (EIS) was performed in PBS (10 mM; pH 7.4) using the AC impedance mode of the CHI660C electrochemical workstation. A perturbation signal of 10 mV was applied across a frequency

range of 0.1 to 1×10^4 Hz. An external Ag/AgCl reference electrode and a platinum mesh auxiliary electrode were utilised. All spectra were recorded at 0 V vs Ag/AgCl and modelled using ZView software (version 3.3e, Scribner Associates, US).

Scanning electron micrographs (SEM) were obtained using a Hitachi S3400V scanning electron microscope at an accelerating voltage of 20 kV. All samples were gold-sputtered for 90 s using a Quorum Technologies sputter coater (750T).

Synthesis of glucose-sensitive hydrogel

The glucose-sensitive hydrogels were prepared by cross-linking Jeffamine® EDR-148 polyetheramine and PEGDGE in DI water. The reaction chemistry is shown in Fig. 1 below. Unless otherwise stated, a 1.0:1.0 molar ratio of PEGDGE to Jeffamine® EDR-148 was utilised with 1% w/w GOx dissolved in the epoxy-amine precursor solution. These precursor solutions were inverted several times until the enzymes were fully dissolved. Where stated, catalase was also incorporated at an enzyme ratio of 9.4 units catalase per unit GOx.

Gravimetric characterisation of the swelling response

The swelling behaviour of the hydrogel was determined gravimetrically. 4 mL of the hydrogel monomer solution was poured into petri-dishes (53 mm internal diameter) and were left at room temperature to cure. Cylindrical gel discs (11.6 mm diameter) were cut from the polymerized hydrogel membrane using a core sampler. Each disc was weighed (W_{dry}) before immersion into the desired aqueous solution. At specific time intervals, the swollen discs were removed from solution, blotted dry and weighed (W_{wet}). The swelling ratio at various time intervals was calculated using the following relationship:

$$\text{Swelling ratio} = \frac{W_{wet} - W_{dry}}{W_{dry}} \quad (3)$$

Statistical analysis was performed on the catalase data using the Analysis ToolPak in Microsoft Excel 2013. Data were compared using an F-test and a T-test with a 95% confidence interval. A value of $p < 0.05$ was considered statistically significant. Electrochemical optimisation of the swelling response

Carbon cloth strips (4 x 1 cm) were cut from a large sheet of carbon cloth. Off-the-shelf nail varnish was applied to the cloth to define the working electrode area (0.5 x 0.5 cm) and prevent solution from travelling up through the cloth via capillary action. The carbon cloth electrodes were then dip-coated into a solution of the hydrogel precursors to apply the hydrogel. When additional coats of hydrogel were required, electrodes were allowed to polymerise for 2 hr between dip-coats to ensure polymerization. Prior to all electrochemical experiments, hydrogel-modified electrodes were swollen in electrolyte solution for 24 hr.

Quantitative analysis of the swelling response

The glucose calibration curve using the gravimetric method was prepared with gel discs containing 5% w/w GOx and catalase

incorporated. Each disc was weighed (W_{dry}) before immersion into distilled water for 24 hr. After 24 hr, each disc was re-weighed (W_{wet}) to quantify the swelling ratio due to water uptake using Equation 3 before immersion into a stirred glucose solution. After 100 min, the swollen discs were removed from solution, blotted dry and weighed (W_{wet}). The swelling ratio due to glucose at 100 min was calculated using Equation 3. The overall swelling response of the gel discs was calculated as follows;

$$\text{Swelling response} = \text{Swelling ratio}_{\text{glucose @ 100 min}} - \text{Swelling ratio}_{\text{water uptake}} \quad (4)$$

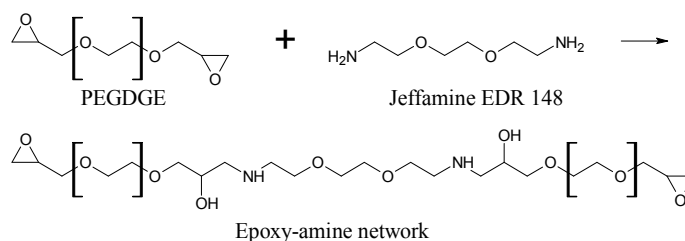


Fig. 1 Hydrogel formation chemistry.

Table 1. Synthesis of amine-epoxy (Jeffamine® EDR-148-PEGDGE) networks.

Mole ratio of amine-epoxy	Jeffamine® EDR-148	PEGDGE	DI H ₂ O
1.2:1.0	0.1129 g	0.3344 g	0.5527 g
1.0:1.0	0.0982 g	0.3491 g	0.5527 g
1.0:1.2	0.0849 g	0.3623 g	0.5527 g
1.0:1.5	0.0706 g	0.3766 g	0.5527 g
1.0:2.0	0.0546 g	0.3882 g	0.5527 g

Results & Discussion

Characterisation of glucose-sensitive hydrogels

The aliphatic diamine was successfully cross-linked with polyethylene glycol diglycidyl ether (PEGDGE) in a single simple polymerization step, generating a polymeric network with pendant basic groups containing immobilised GOx. A series of gels were prepared in which the molar ratio of Jeffamine®:PEGDGE (amine:epoxide) was adjusted as summarised in Table 1.

The relationship between the amine:epoxide molar ratio and the swelling behaviour of the hydrogel in glucose (10 mM) was investigated gravimetrically (Fig. 2). It is evident that the 1.2:1.0 Jeffamine®:PEGDGE network produced the greatest swelling response. This is attributed to the high amount of hydrophilic amines available for ionisation and the low cross-linking density achieved. The swelling response was seen to decrease as the degree of cross-linking increased. The polymer network prepared with a stoichiometric ratio of reactants (1:1)

1 aimed to produce a model network-type structure. A model
2 network is homogeneous and exhibits a known, constant
3 functionality of branch points. Ideally, every polymer chain is
4 connected at each end to different branch points and the cross-
5 linking density is therefore consistent throughout⁴¹. However,
6 real polymer networks tend to deviate from the ideal due to
7 imperfections arising from pre-existing order, inhomogeneities
8 or network defects. Networks formed with an even higher
9 epoxy content, such as 1:1.5 Jeffamine®:PEGDGE and 1:2
10 Jeffamine®:PEGDGE, yielded very poor swelling responses.
11 This behaviour is attributed to the high cross-linking density
12 and poor ionisation. As the network structure becomes tighter,
13 ionisation is impaired by electrostatic effects exerted by
14 adjacent ionised amines. Furthermore, excess epoxy groups can
15 lead to the formation of defects in the network structure in the
16 form of meshes, chain entanglements and grafts⁴² which could
17 possibly restrict the swelling response.

18
19 The influence of several other factors on swelling response
20 were also investigated including the effect of solution stirring,
21 GOx loading and the addition of catalase. These are discussed
22 below.
23
24
25
26
27
28
29
30
31
32
33
34
35
36
37
38
39
40
41
42
43
44
45
46
47
48
49
50
51
52
53
54
55
56
57
58
59
60

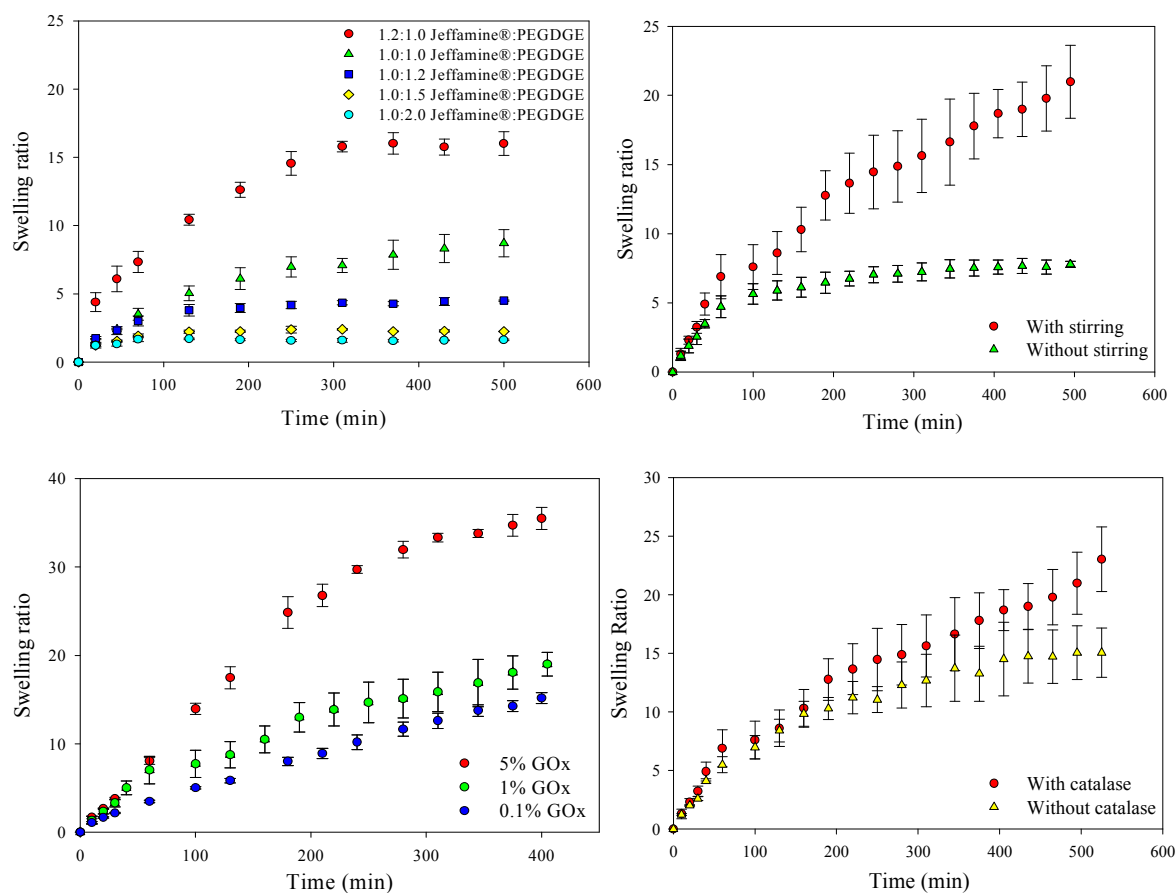


Fig. 2 Swelling behaviour of GOx-modified hydrogel in glucose (10 mM) a) with different amine:epoxy ratios, b) with and without stirring (1% GOx, catalase present), c) containing 0.1 % GOx, 1 % GOx and 5 % GOx in stirred solutions (catalase present) and d) with and without catalase in stirred solutions (1% GOx). (n=3, average response \pm standard deviation)

Optimum enzyme kinetics are paramount for achieving good response times in enzyme-based biosensors. Fig. 2b shows the effect of solution stirring on the swelling behaviour of glucose-sensitive hydrogels. Stirring, as expected, can be seen to dramatically accelerate the enzyme kinetics. After 100 min, the swelling response has risen 35% in the stirred solutions compared with the unstirred solutions. This increases further to 187% after 500 min. It is evident that without stirring, GOx activity is diffusion limited. Under stagnant conditions, the system relies upon the mass transport of glucose molecules to the gel surface by natural diffusion governed by Fick's first law. Additionally, an external diffusion layer (Nernst diffusion layer) can be present at the surface in which concentration polarisation occurs, whereby the solution at the membrane surface becomes depleted in the permeating solute and enriched in this solute on the permeate side. The mechanical agitation produces forced convection in the surrounding solution. This reduces the thickness of the diffusion layer which is known to be dependent on the nature and stirring speed of the solution, with more rapid stirring corresponding to a thinner diffusion layer⁴⁰. Consequently, the

collision frequency of GOx with substrate molecules is increased, thereby improving the hydrogel response time.

Enzyme loading was investigated by preparing GOx-modified hydrogels in which the GOx loading was varied from 0.1% to 5% total enzyme (GOx and catalase). The ratio of catalase:GOx content was held constant, to optimise the GOx loading. The swelling response to glucose (10 mM) is displayed in Fig. 2c. Substrates and product can diffuse in and out of the gel network whilst the enzyme, which is immobilised via matrix entrapment is retained due its large size. Additionally, as the isoelectric point of GOx is 4.2⁴³ the surface of the enzyme is negatively charged when the hydrogel is swollen in DI water or in PBS and thus, the enzyme may also be retained by ionic interactions with the cationic polymer network. It was observed that as the enzyme loading was increased from 0.1% to 5%, the swelling response to glucose substrate increased. After 100 min the swelling ratio increased by almost 3-fold, from 5 ± 0.118 to 14 ± 0.637 . This is due to each GOx molecule functioning as a reaction site for the catalysed oxidation of glucose into gluconic acid. Therefore, a higher GOx content leads to a greater production of gluconic acid, increasing ionisation of the polymeric network and hence the swelling capacity. A similar

behaviour has been reported previously whereby GOx activity increased in poly(2-hydroxyethyl methacrylate) (HEMA) hydrogel membranes upon increasing the GOx loading up to 15-20 mg per gram of gel^{41,42}.

Finally, the swelling behaviour of glucose-sensitive hydrogels with and without immobilized catalase was studied (Fig. 2d). As can be seen in Fig. 2d, greater swelling responses are achieved for the hydrogels that have catalase incorporated. This differentiation in the swelling responses becomes significant after 160 min ($p < 0.05$). It is likely at this time, that the oxygen supply is beginning to deplete and the concentration of hydrogen peroxide is increasing in the gels without catalase, inhibiting glucose catalysis and hence restricting the swelling response. After 525 min in glucose, hydrogels without catalase produced a swelling ratio of 15 ± 2.12 whereas gels with catalase resulted in a response of 23 ± 2.75 , an increase of 65%. Additionally, after 525 min of swelling, gels with immobilised catalase are continuing to swell while those without are reaching steady-state. This corresponds with the increased oxygen supply and improved glucose oxidase stability by the removal of hydrogen peroxide via the catalase reaction.

Electrochemical optimisation of glucose-sensitive hydrogels

As an alternative to measurement of the swelling gravimetrically, we investigated if the swelling response could be monitored electrochemically. Carbon cloth was selected as an electrode material that is porous and conformable - properties that can facilitate the hydrogel swelling. Carbon cloth consists of woven graphitised carbon fibres prepared from spun yarn. With a carbon content of 99%, the fabric has the electrochemical properties of other carbon-based electrodes i.e. high electric conductivity, gas permeability, corrosion resistance and high tensile strength⁴⁴.

Fig. 3 depicts SEM images of bare carbon cloth (a-b), 1 coat (c-d), 2 coats (e-f) and 5 coats (g-h) of hydrogel applied via dip-coating into a hydrogel precursor solution. As the electrode material is porous, hydrogel polymerisation occurs three-dimensionally with the hydrogel penetrating the cloth fibres instead of only coating the surface. The numerous individual fibres are evident in images (a) and (b) showing a high surface area. This is advantageous in an electrode material as it can produce high responses due to the increased surface area of electroactive material. Images (c) and (d) show that 1 coating of gel is sufficient to coat all the fibres of the cloth (15 mm thick). As the loading of gel was increased, the topography became smoother and, after 5 coats, the individual carbon fibres were no longer visible (Fig. 3, e,f).

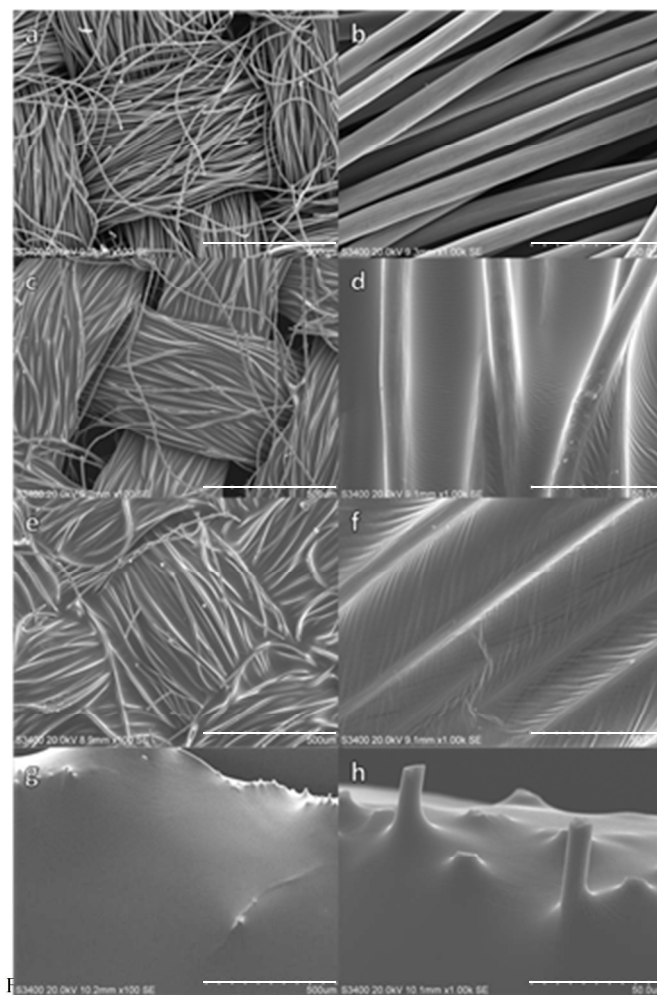


Figure 3. SEM images of bare carbon cloth (a-b), 1 coat (c-d), 2 coats (e-f) and 5 coats (g-h) of hydrogel applied via dip-coating into a hydrogel precursor solution. The right-hand column contains the low magnification (100 X) images (500 μm scale bars) and the left-hand column contains the high magnification (1000 X) images (50 μm scale bars) (a)-(b) bare carbon cloth electrode, (c)-(d) 1 coat of gel, (e)-(f) 2 coats of gel and (g)-(h) 5 coats of gel.

The voltammetric performance of the hydrogel-modified carbon cloth was explored using the ferri/ferrocyanide redox couple. CVs of the redox couple at the bare carbon cloth and with a number of hydrogel coatings were recorded (Fig. 4). The thickness of the hydrogel layer had a profound effect on the voltammetric properties of the carbon cloth. The peak potential separation (ΔE_p) increased and the anodic ($i_{p,a}$) and cathodic ($i_{p,c}$) peak currents decreased, as increasing numbers of coats of hydrogel precursors were applied. 5 coats of hydrogel completely inhibited the redox probe from accessing the electrode surface over the timescale of the experiment. This behaviour was attributed to the very thick hydrogel film (Fig. 3,g,h) which impeded the diffusion of the redox probe to the electrode surface. The electrode with a single coat of gel demonstrated a linear dependence on the square root of scan rate (v)^{1/2}, ($r^2 = 0.9928$, data not shown), suggesting a diffusion controlled process was occurring through the hydrogel.

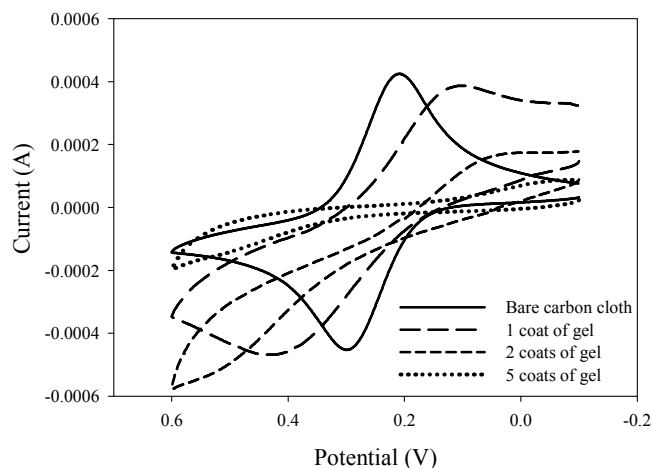


Fig. 4 Cyclic voltammograms of different hydrogel loadings on carbon cloth electrodes in potassium ferrocyanide (2 mM) in KCl (1 M).

Non-faradaic EIS was employed as an alternate means to track hydrogel swelling. Fig. 5 represents typical Nyquist ($-Z''$ vs. Z') plots for the hydrogel-modified carbon cloth electrodes with a single coat of gel applied. The Nyquist impedance spectra show the relationship between the real and imaginary components of complex impedance of the hydrogel in response to glucose induced swelling. The spectra are dominated by the presence of capacitive lines. They comprise a high frequency intercept on the real Z' axis and the beginning of a semi-circular arc across the high to low frequency range. The high frequency intercept is representative of a combination of electrolyte ionic resistance and the resistance of the contacts to the potentiostat. The semi-circular arc, which becomes more visible with increasing glucose concentration, corresponds primarily to changes in capacitance and resistance at the electrode interface.

It is evident that swelling of the hydrogel alters the capacitance and diffusional properties of the gel network. The

imaginary part of the impedance ($-Z''$) decreases with increasing concentrations of glucose suggesting an increase in capacitance and decrease in gel resistance. This decrease in $-Z''$

is attributed to the transition of the hydrogel network from a compressed state to an expanded state via ionisation of the polymer backbone and increased osmotic pressure. Thus, hydrogel porosity increases and the diffusion rate through the gel network is accelerated. Fig. 6 shows combined Bode plots of the modulus of impedance (Z) and the phase curve (ϕ) of the GOx hydrogels as a function of the frequency range scanned.

They can be divided into frequency regions indicative of the dominant kinetics within that domain. The horizontal domain at high frequencies (>0.4 kHz) with low phase shows resistive behaviour, while the mid-frequency domain (100 Hz to 0 Hz) shows the capacitive behaviour of the hydrogel in the form of line with a slope of -1, with a phase of -80 degrees and finally, the low frequency domain (<0 Hz) where the capacitive behaviour persists. Z is seen to decrease with increasing glucose concentration across the frequency region, resulting again from the increase in the porosity of the hydrogel via

ionization-induced swelling.

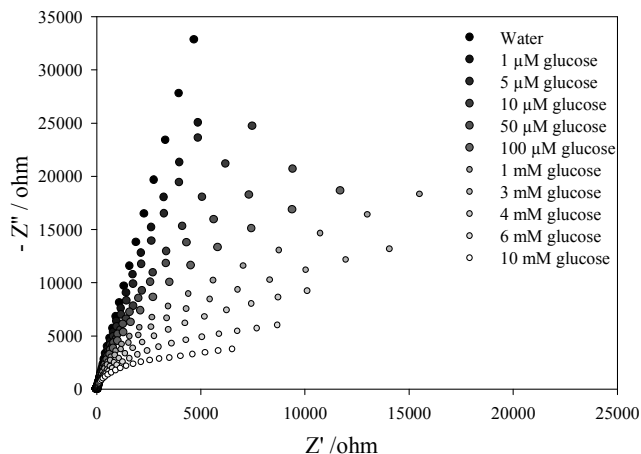


Fig. 5 Nyquist plot of GOx-modified hydrogels after swelling in various concentrations of glucose for 24 hr (in 10 mM PBS).

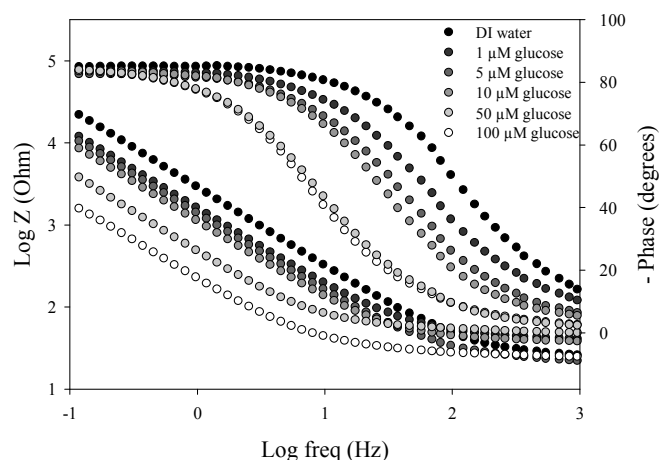


Fig. 6 Bode plots showing impedance of GOx hydrogels after swelling in various concentrations of glucose for 24 hr (in 10 mM PBS).

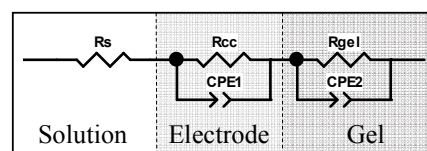


Fig. 7 Electrical equivalent circuit used to fit EIS spectra.

Quantitative glucose analysis

The swelling response of the optimised hydrogel in glucose was quantitatively tracked using both gravimetry and EIS (both calibration curves are present in the Electronic Supplementary Information). Utilising gravimetry, the swelling response of glucose-sensitive hydrogel discs was linear in the range 1 to 20 mM glucose (18-360 mg/dL) with a correlation coefficient of 0.9946 and detection limit of 0.33 mM. This detection limit was calculated based on the swelling response of hydrogel discs in DI water. This response was equated to 0.33 mM using the

equation of the line generated by the calibration curve with three times the standard deviation added. Hydrogels without GOx incorporated were also swollen in glucose (10 mM) to verify that glucose alone was not altering the swelling response. Hydrogels in the presence of glucose produced a swelling profile equivalent to hydrogels swollen in water indicating that glucose was not interacting with the polymer network (data not shown).

A second calibration curve was prepared based on the impedimetric data. EIS can distinguish the individual contributions of each circuit component by modelling the data using an electrical equivalent circuit representative of the system under investigation. The circuit displayed in Fig. 7 produced the best fit to the experimental data. It is a simple circuit that can be divided up by its individual elements. It comprises the solution resistance (R_s) in series with a parallel combination of a constant phase element (CPE1) and the intrinsic resistance of the carbon cloth substrate (R_{cc}), connected in series to a CPE (CPE2) and resistance (R_{gel}) from the hydrogel coating. CPEs were utilised in lieu of pure capacitors to compensate for non-homogeneity in the system. They are sometimes referred to as 'leaky' capacitors and are a realistic model for rough, porous materials such as these^{45, 46}. A linear decrease in gel resistance (R_{gel}) corresponding to the swelling response was detected in the range 1 to 100 μM with a correlation coefficient of 0.9980 and a detection limit of 0.08 μM . The limit of detection was calculated based on the swelling response of GOx-modified hydrogels in PBS (10 mM). The average R_{gel} value of the hydrogel-modified carbon cloth electrodes in PBS equated to 0.08 μM using the equation of the line generated by the calibration curve with three times the standard deviation added.

In comparison with the gravimetric method, the linear range has increased by three orders of magnitude and the limit of detection by six orders of magnitude using EIS. This substantial increase in sensitivity introduces the possibility of measuring glucose concentration in sweat or ISF - a much less invasive approach to glucose monitoring than blood measurements. Indeed, electrochemical transduction would have significant advantages given its reliability, simplicity and facile coupling with low-cost microelectronics. The choice of a conducting textile opens up the possibility of a wearable glucose sensor, whereas gravimetric measurements are not practical for biosensing, particularly in the area of wearable sensors. As shown in Table 2 the linear range and limit of detection of this work compare favourably with other low glucose concentration biosensors targeting skin analysis.

Table 2. Linear range and limit of detection comparison with other low glucose concentration biosensors for skin analysis.

Sensor	Principle	Linear Range	Limit of Detection
GOx-Prussian Blue amperometric biosensor ⁴⁷	Temporary tattoo-based system which uses reverse iontophoresis to extract ISF	0-100 μM	3 μM
GOx-Carbon nanotubes	3-electrode transducer which uses reverse iontophoresis to	3-15 mM	*3 mM

amperometric biosensor ⁴⁸	extract ISF		
GOx-Ferrocene amperometric biosensor ⁴⁹	3-electrode transducer which uses reverse iontophoresis to extract ISF	3-15 mM	*3 mM
Fluorophore-labelled glucose binding protein ⁵⁰	Fluorescence intensity decreases with increasing glucose concentration (Unspecified biological matrix)	0-5 μM	0.08 μM
This work	Hydrogel swelling	1-100 μM	0.08 μM

*In absence of limit of detection lowest standard concentration is given.

Conclusions

This paper demonstrates a rapid, facile, single step method for the fabrication of a glucose-sensitive hydrogel. The 3D nature of the polymer network allowed a high enzyme loading in a biocompatible environment. Initial characterisation of the swelling response using weight-based swelling studies determined that the response could be tailored by variation of the cross-linking density of the network and the enzyme loading. Additionally, the thickness of the hydrogel coating on the carbon cloth had a great impact on its voltammetric properties and suggested a diffusion controlled process was occurring through the hydrogel. EIS measurements showed a decrease in impedance with increasing glucose concentration.

Both gravimetry and EIS were used as quantitative approaches to measure the swelling effect of glucose on these gels. Direct gravimetric measurement gave a sensitivity down to 0.33 mM glucose. In this case of EIS, the limit of detection improves dramatically by approx. 6-fold. This provides strong evidence that non-faradaic EIS can be used to sensitively track hydrogel swelling in response to a target analyte.

This work establishes for the first time, a simple approach for developing impedimetric biosensors based on the swelling of stimuli-responsive hydrogels. Possible interference effects remain to be explored, including common organic acids found in sweat such as lactic and pyruvic acid. While the swelling of bulk gels is slow, it is likely that this time will be significantly reduced as the thickness of the gel layers and the scale of the electrodes is reduced. The volume of sample required for analysis will also be reduced following this miniaturisation, providing a viable method for glucose monitoring in wearable sweat or ISF sensors.

Acknowledgements

The authors wish to thank the Irish Research Council for financial assistance provided under the 'EMBARC initiative'. The authors also gratefully acknowledge funding from Science Foundation Ireland under the Walton Fellowship Scheme (11/W.1/B1950).

Notes and references

^a National Centre for Sensor Research, Dublin City University, Dublin 9, Ireland. E-mail: nicky.mackenna2@mail.dcu.ie

^b Bioengineering, University of Massachusetts Dartmouth, Dartmouth, USA.

- † Electronic Supplementary Information (ESI) available: [details of any supplementary information available should be included here]. See DOI: 10.1039/b000000x/
1. M. Sirousazar and M. Kokabi, *Intelligent Nanomaterials*, Scrivener Publishing LLC, Massachusetts, 2012.
 2. N. A. Peppas, P. Bures, W. Leobandung and H. Ichikawa, *Eur. J. Pharm. Biopharm.*, 2000, **50**, 27-46.
 3. H. Hezaveh and Muhamad, II, *Chem. Eng. Res. Des.*, 2013, **91**, 508-519.
 4. L. Klouda and A. G. Mikos, *Eur. J. Pharm. Biopharm.*, 2008, **68**, 34-45.
 5. C. W. Lo, D. F. Zhu and H. R. Jiang, *Soft Matter*, 2011, **7**, 5604-5609.
 6. B. F. Ye, Y. J. Zhao, Y. Cheng, T. T. Li, Z. Y. Xie, X. W. Zhao and Z. Z. Gu, *Nanoscale*, 2012, **4**, 5998-6003.
 7. D. Arunbabu, A. Sannigrahi and T. Jana, *Soft Matter*, 2011, **7**, 2592-2599.
 8. J. H. Holtz and S. A. Asher, *Nature*, 1997, **389**, 829-832.
 9. A. Doring, W. Birnbaum and D. Kuckling, *Chemical Society Reviews*, 2013, **42**, 7391-7420.
 10. Y. Wang, A. J. Dong, Z. C. Yuan and D. J. Chen, *Colloid Surf. A-Physicochem. Eng. Asp.*, 2012, **415**, 68-76.
 11. Y. Liu, A. Servant, O. J. Guy, K. T. Al-Jamal, P. R. Williams, K. M. Hawkins and K. Kostarelos, *Sensor Actuat B-Chem*, 2012, **175**, 100-105.
 12. K. Gawel and B. T. Stokke, *Soft Matter*, 2011, **7**, 4615-4618.
 13. L. L. Li, X. D. Xing and Z. L. Liu, *Journal of Applied Polymer Science*, 2012, **124**, 1128-1136.
 14. Q. B. Wei, Y. L. Luo, F. Fu, Y. Q. Zhang and R. X. Ma, *Journal of Applied Polymer Science*, 2013, **129**, 806-814.
 15. V. P. S. Nykanen, A. Nykanen, M. A. Puska, G. G. Silva and J. Ruokolainen, *Soft Matter*, 2011, **7**, 4414-4424.
 16. G. R. Hendrickson and L. A. Lyon, *Soft Matter*, 2009, **5**, 29-35.
 17. I. Tokarev and S. Minko, *Soft Matter*, 2009, **5**, 511-524.
 18. K. Gawel, D. Barriet, M. Sletmoen and B. T. Stokke, *Sensors-Basel*, 2010, **10**, 4381-4409.
 19. A. Richter, G. Paschew, S. Klatt, J. Lienig, K. F. Arndt and H. J. P. Adler, *Sensors-Basel*, 2008, **8**, 561-581.
 20. V. P. Zanini, B. L. de Mishima and V. Solis, *Sensor Actuat B-Chem*, 2011, **155**, 75-80.
 21. J. Bunsow, A. Enzenberg, K. Pohl, W. Schuhmann and D. Johannsmann, *Electroanalysis*, 2010, **22**, 978-984.
 22. S. Brahim and A. Guiseppi-Elie, *Electroanalysis*, 2005, **17**, 556-570.
 23. S. Brahim, A. M. Wilson, D. Narinesingh, E. Iwuoha and A. Guiseppi-Elie, *Microchim. Acta*, 2003, **143**, 123-137.
 24. S. Brahim, D. Narinesingh and A. Giuseppe-Elie, *Electroanalysis*, 2002, **14**, 627-633.
 25. H. F. Cui, J. S. Ye, W. D. Zhang and F. S. Sheu, *Biosens Bioelectron*, 2009, **24**, 1723-1729.
 26. M. Niculescu, S. Sigina and E. Csoregi, *Anal. Lett.*, 2003, **36**, 1721-1737.
 27. H. M. Liu, C. X. Liu, L. Y. Jiang, J. Liu, Q. D. Yang, Z. H. Guo and X. X. Cai, *Electroanalysis*, 2008, **20**, 170-177.
 28. L. Montero, G. Gabriel, A. Guimera, R. Villa, K. K. Gleason and S. Borros, *Vacuum*, 2012, **86**, 2102-2104.
 29. A. Suri, R. Campos, D. G. Rackus, N. J. S. Spiller, C. Richardson, L. O. Palsson and R. Katakya, *Soft Matter*, 2011, **7**, 7071-7077.
 30. C. M. Weikart, Y. Matsuzawa, L. Winterton and H. K. Yasuda, *J. Biomed. Mater. Res.*, 2001, **54**, 597-607.
 31. M. G. Mahjani, A. Ehsani and M. Jafarian, *Synthetic Met.*, 2010, **160**, 1252-1258.
 32. R. Gabai, N. Sallacan, V. Chegel, T. Bourenko, E. Katz and I. Willner, *The Journal of Physical Chemistry B*, 2001, **105**, 8196-8202.
 33. B. Beier, K. Musick, A. Matsumoto, A. Panitch, E. Nauman and P. Irazoqui, *Sensors-Basel*, 2011, **11**, 409-424.
 34. C. Zhang, M. D. Losego and P. V. Braun, *Chemistry of Materials*, 2013, **25**, 3239-3250.
 35. A. Matsumoto, T. Kurata, D. Shiino and K. Kataoka, *Macromolecules*, 2004, **37**, 1502-1510.
 36. Y. J. Lee, S. A. Pruzinsky and P. V. Braun, *Langmuir*, 2004, **20**, 3096-3106.
 37. T. Miyata, A. Jikihara, K. Nakamae and A. S. Hoffman, *Journal of Biomaterials Science -- Polymer Edition*, 2004, **15**, 1085-1098.
 38. R. Zhang, M. Tang, A. Bowyer, R. Eisenthal and J. Hubble, *React. Funct. Polym.*, 2006, **66**, 757-767.
 39. R. Yin, K. Wang, J. Han and J. Nie, *Carbohydr. Polym.*, 2010, **82**, 412-418.
 40. S. H. Jeong, K. T. Oh and K. Park, *Polymeric Biomaterials: Medicinal and Pharmaceutical Applications, Volume 2*, CRC Press, Florida, 2013.
 41. G. Hild, *Progress in Polymer Science*, 1998, **23**, 1019-1149.
 42. N. A. Peppas, *Hydrogels in Medicine and Pharmacy: Fundamentals*, CRC Press, 1986.
 43. S. Palanisamy, A. T. E. Vilian and S.-M. Chen, *International Journal of Electrochemical Science*, 2012, **7**, 2153-2163.
 44. M. M. Barsan, R. C. Carvalho, Y. Zhong, X. Sun and C. M. A. Brett, *Electrochimica Acta*, 2012, **85**, 203-209.
 45. W. G. Pell, A. Zolfaghari and B. E. Conway, *Journal of Electroanalytical Chemistry*, 2002, **532**, 13-23.
 46. J. Li, Q. Yang and I. Zhitomirsky, *Nanoscale Research Letters*, 2010, **5**, 512-517.
 47. A. J. Bandodkar, W. Jia, C. Yardimci, X. Wang, J. Ramirez and J. Wang, *Anal Chem*, 2014, **87**, 394-398.
 48. T. P. Sun, H. L. Shieh, C. T. S. Ching, Y. D. Yao, S. H. Huang, C. M. Liu, W. H. Liu and C. Y. Chen, *International Journal of Nanomedicine*, 2010, **5**, 343-349.
 49. C. T. S. Ching, T. P. Sun, S. H. Huang, H. L. Shieh and C. Y. Chen, *Annals of Biomedical Engineering*, 2010, **38**, 1548-1555.
 50. Y. Kostov, X. D. Ge, G. Rao and L. Tolosa, *Measurement Science & Technology*, 2014, **25**.